

# The mineralogy and genesis of uranium in rhyolitic ignimbrites of Precambrian age from Duobblon, Sweden

JOHN A. T. SMELLIE

Geological Survey of Sweden, Box 801, Luleå, Sweden

**ABSTRACT.** The Duobblon rhyolitic ignimbrites, of middle Precambrian age are 60 m thick. They consist of at least three flows with varying degrees of welding and have undergone devitrification, producing lithophysal and spherulitic textures. They are overlain by thick fluvialite red-bed-type conglomerates and sandstones, which in turn are capped by terrestrial acid volcanics.

Uranium enrichments of up to 3000 ppm U occur within two or three peneconcordant tabular horizons which are mostly lithophysae-bearing. Fission-track investigations of the ignimbrites and overlying conglomerates and sandstones, which supplement earlier mineralogical studies, show that U occurs as fine pitchblende disseminations; as complex uranotitanates associated with Fe-Ti-Mn oxides; and as coatings associated with matrix sericite. Small amounts of U are present in such primary accessory minerals as sphene, apatite, and zircon.

It is suggested that oxidizing U-bearing solutions, generated partly during devitrification of the ignimbrites and partly from the overlying volcano-sedimentary pile, produced the U enrichments with later sulphide deposition, along the more permeable lithophysal horizons in the ignimbrites.

THE Precambrian rhyolitic ignimbrites of the Duobblon area (figs. 1 and 2), previously described by Einarsson (1979) and Lindroos and Smellie (1979), are composed of welded and partially welded rhyolites and tuffs of ash-fall and ash-flow origin. The ignimbrite unit is some 60 m thick and 4 to 5 km in strike length, comprising three main flows each separated by a thin conglomeratic bed which varies in thickness from 1 to 10 m. The basal flow has the greatest areal extent and the whole unit thins out laterally eastwards.

The ignimbrites contain relatively high U concentrations for such rocks with an average of 200-300 ppm U and with localized concentrations reaching 3000 ppm U. They occur within two or three peneconcordant tabular horizons 5 to 25 m thick and more than 1000 m long. The mineralization is not confined to any single flow, although

the highest U concentrations tend to be associated with the basal member. From the literature, the Buckshot Ignimbrite of late Eocene to early Oligocene age (Anderson, 1975), and the pyroclastic acid tuffs of Permian age at Novazza (Guarascio, 1976), are the only published occurrences containing such high levels of U.

Acid volcanics, which contain on average 5 to 7 ppm U and 20 to 30 ppm Th, are considered by many workers to be important source rocks of U, and their investigations have tended to emphasize the post-depositional mobilization of the U. Investigations by Rosholt and co-workers (1969, 1971), Shatkov *et al.* (1970), and Zielinski and co-workers (1977, 1978, 1980), indicate that crystalline rhyolites (felsites) tend to be depleted in U in contrast to co-existing non-hydrated glasses (obsidian) or hydrated glasses (perlite), and there are also indications that U depletion increases with age at a rate which depends on whether the rhyolites are per-alkaline (fastest) or calc-alkaline (slowest). The Duobblon ignimbrites, being Precambrian in age and having undergone post-depositional devitrification and recrystallization, are therefore somewhat exceptional in containing such high levels of U. Lindroos and Smellie (1979) have previously described aspects of the U distribution in the ignimbrites. The present paper presents a detailed mineralogical and fission-track study of U distribution, together with additional chemical data. The overlying tuffitic sandstone and conglomeratic units which have probably contributed to the total U content of the underlying volcanics are also considered.

## *Geological setting*

The geology of the Duobblon area (figs. 1 and 2) has been described in detail by Einarsson (1970, 1979) and by Lindroos and Smellie (1979). Briefly, the rocks are of middle Precambrian age situated

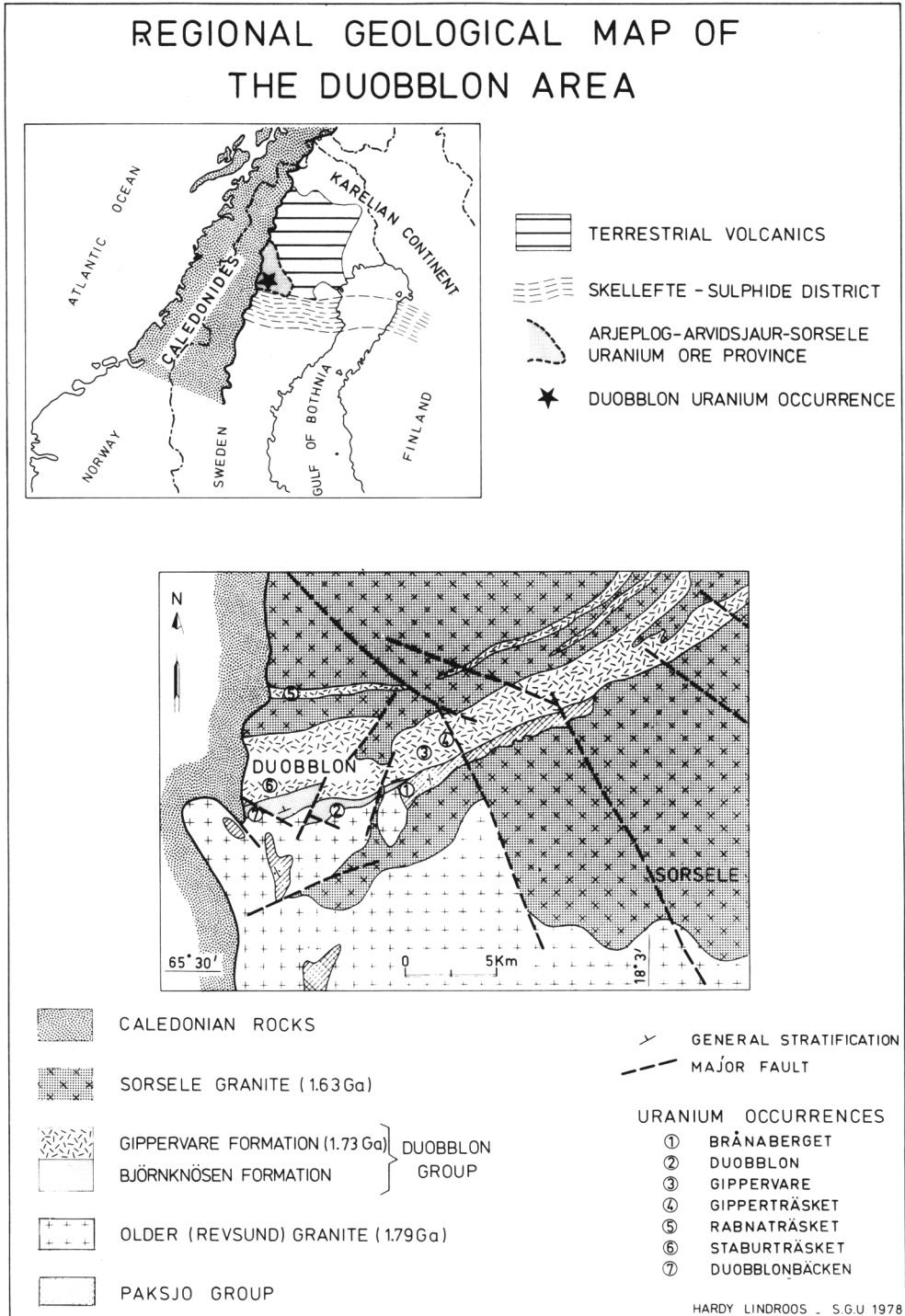


FIG. 1. Generalized map of the Duobblon area, northern Sweden. Location map (top) shows position of the Duobblon U occurrence within the Arjeplog-Arvidsjaur-Sorsele U ore province (after Lindroos and Smellie, 1979).

near an important structural boundary of the Baltic Shield which separates a northern continent from a southern oceanic region in Svecofennian times (2.00-1.75 Ga). The geology comprises the Paksjo and Duobblon groups together with the Revsund granite and the younger Sorsele granite masses. The Duobblon group consists of rhyolitic ignimbrites and an underlying basal breccia, which westwards lie unconformably on a deeply weathered granite basement (correlated with the Revsund granite) of about 1.75 Ga. To the east, graphitic schists of the Paksjo group form the basement to the ignimbrite flows which themselves thin out eastwards, suggesting a volcanic source to the north-west concealed by the Caledonian allochthon.

The ignimbrites are overlain by thick fluvial deposits of red-bed-type conglomerates and sandstones, which are in turn capped by acid to intermediate terrestrial volcanics. The younger granite, known as the Sorsele granite and dated at 1.59 Ga (Welin *et al.*, 1971; Welin, 1980), occurs to the north of the Duobblon area and is intrusive into the other rock units.

*Major features of the distribution of U*

The Duobblon U occurrence (fig. 1) is located at the periphery of the Arjeplog-Arvidsjaur-Sorsele U province (Adamek and Wilson, 1979). The most important U occurrences in the province are believed to be epigenetic, in contrast to Duobblon which is later and considered to be syngenetic and possibly also related to devitrification (Lindroos and Smellie, 1979). Within the Duobblon group (fig. 2), U mineralization has been found associated with all members of the group and also with schists of the Paksjo group. The most important concentrations in the Duobblon group occur in the lithophysae-bearing rhyolitic ignimbrites of the Björnknösen Formation, the highest concentrations occurring in an area between a basement high and the intersection of two erosion surfaces which form the base of the overlying sandstone-conglomerate units. The interbedded and overlying polymict conglomerates contain minor local enrichments (100 to 1000 ppm U) in contrast to the underlying basal breccia and the schists of the Paksjo group. The U content

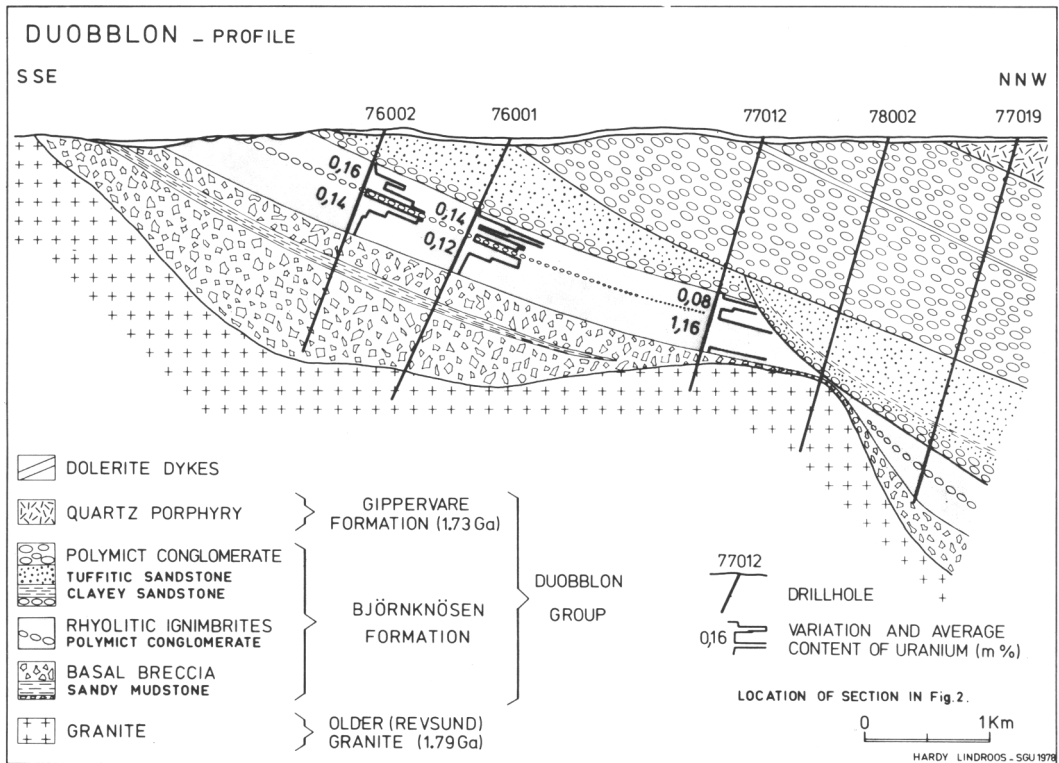


Fig. 2. Vertical cross-section through the Duobblon U occurrence. Studied samples were collected from drill-cores 76001, 76002, 77012, and 78013 (after Lindroos and Smellie, 1979).

decreases markedly towards the erosion surface which truncates the lithophysal unit.

#### *Petrology of the ignimbrites*

*General aspect.* Some aspects of the mineralogy have been described by Einarsson (1979) and in more detail by Lindroos and Smellie (1979). The ignimbrites, consisting of ash-fall and ash-flow tuffs with rhyolitic lavas, have been partly or completely welded and subsequently devitrified. Modal analyses for welded, partly welded, and non-welded porphyritic tuffs are compared in Table I. Changes in welding through the ignimbrite unit probably reflect different flows.

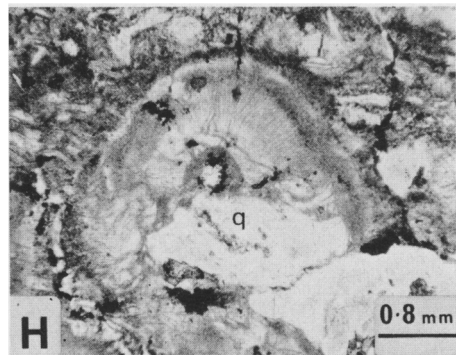
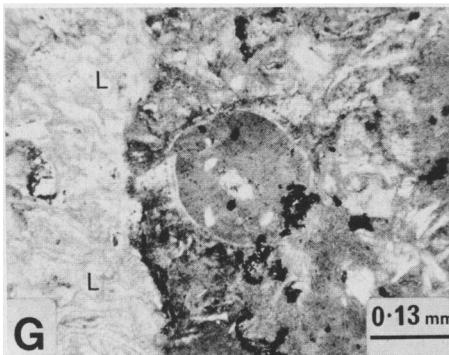
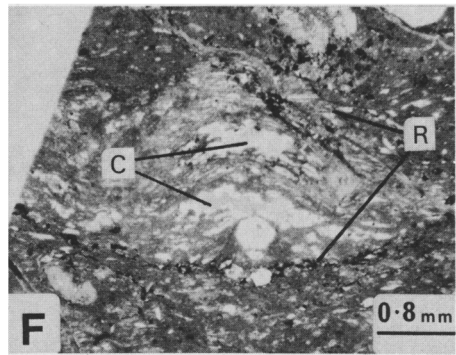
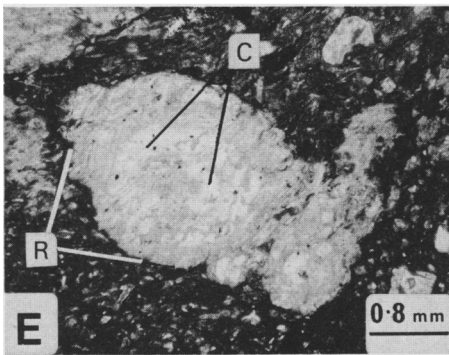
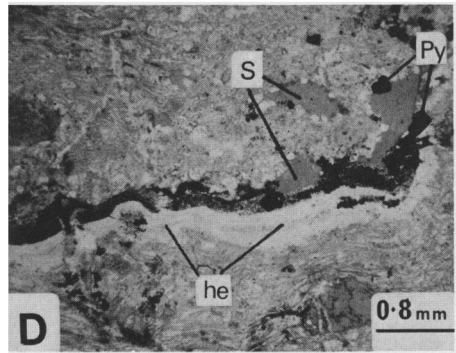
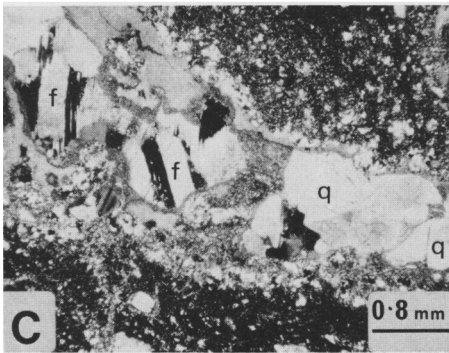
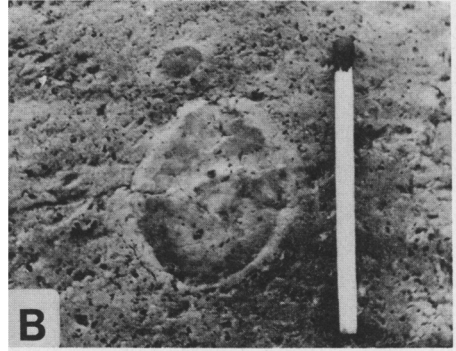
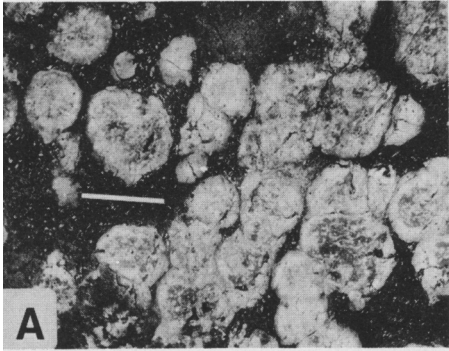
The welded portions of the ignimbrites vary in colour from dark olive-green through several shades of grey to pink and reddish brown corresponding to a sericite-rich and felsitic matrix, and a matrix with disseminated hematite respectively. Microscopically, the partly welded tuff horizons preserve many primary pyroclastic features including partly consolidated pumice fragments, volcanic ash, and rock fragments (1 to 4 mm in size). More commonly, however, these features have been almost obscured by varying degrees of welding and devitrification (e.g. Ross and Smith, 1961; Lilljequist and Svensson, 1974).

TABLE I. *Modal analyses of welded (A), non-welded (B), and partially welded (C) porphyritic tuffs from the Duobblon ignimbrites*

	A	B	C
Felsite matrix	80.7	80.3	79.0
Quartz phenocrysts	6.0	2.8	2.0
Albite phenocrysts	9.2	8.0	6.3
Fe-Ti-Mn-oxides	3.6	4.8	3.6
Fragments (pumice etc.)	0.5	4.1	9.1
	100.0	100.0	100.0
No. of samples	5	5	6
No. of points counted/ sample	1500	1500	1500

Feldspar and quartz phenocrysts are common throughout the ignimbrites and eutaxitic porphyry structures are abundant (fig. 5C). The feldspar phenocrysts (0.3 to 5.0 mm in diameter) are sub-hedral consisting mainly of albite. They have usually undergone some sericitization and resorption, and the quartz phenocrysts of similar size range show resorption in the rounding of edges and embayment features.

FIG. 3. Textural and mineralogical characteristics of lithophysae and spherulites within the Duobblon ignimbrites. A. Lithophysae of varying sizes and degrees of coalescence within a porphyritic matrix rich in U and sericite. B. Detail of a lithophysa showing how growth has been superimposed on the rock fabric. Note that the distribution of quartz and plagioclase phenocrysts and Fe-Ti-Mn oxides is similar within and surrounding the lithophysa. The light-coloured marginal rim to the lithophysa is typical and generally consists of quartz or a quartz-feldspar aggregate. Concentric growth patterns can also be distinguished within the lithophysa. C. Lithophysal cavity infillings composed mainly of twinned plagioclase feldspar (f) and quartz aggregates (q) together with subordinate amounts of granular quartz, calcite, sericite, sulphides (usually pyrite with subsidiary chalcopyrite), and small concentrations of epidote and chlorite. Plane polarized light. Specimen 7672:003. D. Lithophysal cavity infillings characterized by layers of pyrite idiomorphs (Py) together with fine granular quartz bands containing alternations of disseminated pyrite (sometimes associated with chlorite and epidote) and hematite (he). Adjacent are small cavity infillings of sericite (s). The remainder of the lithophysal interior shows typical eutaxitic textures. Plane polarized light. Specimen 7672:163. E. Compound lithophysae formed by the coalescence of several small growth nuclei. Note within the large lithophysa the concentric form of the cavities (C) and the preservation of the welded eutaxitic structures, the quartz and plagioclase phenocrysts, and the Fe-Ti-Mn oxides (dark spots). The interiors of the lithophysae are lightly sericitized in contrast to the heavily sericitized matrix. Forming a dark rim (R) to the lithophysae are opaques consisting mainly of magnetite and hydroxy iron oxides; magnetite also occurs as disseminations within the matrix. Plane polarized light. Specimen 7672:164. F. Lensoid-shaped lithophysa exhibiting how growth has partly been due to expansion and rupture along compaction planes. The resulting cavities (C) are bordered by quartz aggregates with the central cavity area infilled by sericite. Note again the peripheral rim (R) of opaques demarcating the lithophysal edge. Plane polarized light. Specimen 7672:061. G. Spherulite showing nucleation around a central quartz aggregate and the incorporation of quartz and feldspar phenocrysts together with Fe-Ti-Mn oxides. Fine radial quartz and sericite constitute most of the spherulitic interior; the sericite probably representing the alteration products of primary orthoclase growth lamellae. The light area to the left of the spherulite is a lithophysa (L). Plane polarized light. Specimen 7672:001. H. Spherulite exhibiting nucleation around a central quartz fragment or phenocryst and the almost complete incorporation of a large quartz fragment (q). The radially orientated quartz and sericite cross-cuts the primary eutaxitic textures which remain as ghost imprints within the spherulite. Concentric haloes of opaque dustings probably represent an advancing mafic-rich solution front during spherulite growth. Plane polarized light. Specimen 7672:061.



Welded pumice, ash, and glass shard particles are commonly present as matrix minerals and generally persist as ghost imprints after devitrification. More usually the matrix consists solely of a devitrified dense felsitic mass (< 0.1 mm size range of individual grains) composed of residual feldspar (now mostly altered to sericite) and quartz (cristobalite?) together with minor titanomagnetite, ilmenite, magnetite, apatite, sphene, epidote, calcite, pyrite, and zircon. These accessory minerals are common in various combinations throughout the ignimbrites.

A marked feature of the ignimbrites is the presence, within certain welded horizons, of lithophysal and vapour-phase cavities which may be drusy but are more commonly filled with late-stage vapour-phase crystals. Spherulitic textures (up to 4 mm in diameter) are sporadic, exhibiting typical radial growth structures nucleated mostly around quartz fragments (fig. 3G, H). The welded shard textures are usually well preserved, although the growth of spherulites cuts across the shard alignment. Single spherulites are often surrounded by cloudy grey, sometimes brown, haloes which also

occur as concentric zones within them. These haloes have been attributed to a solution front (Anderson, 1975) and probably contain oxidized iron or titanium or both, from the breakdown of titanomagnetite to rutile or anatase. The concentric arrangements may represent different rates of growth.

In contrast to the spherulites, the lithophysae formed around local centres of crystallization which probably included small bubbles or intra-granular volatile-rich cavities. During development of the lithophysae, the accumulation of volatiles that exsolved from the volcanic glass during devitrification exerted a pressure which, combined with the shrinkage of the enclosing material during cooling, forced the walls of the cavity outwards, expansion being by rupture along flow or compaction planes (fig. 3F). The resulting cavities are filled by coarse quartz, albite, calcite, chlorite, muscovite, and pyrite (fig. 3C, D). These central cavities, however, often constitute only a small proportion of the lithophysae; the greater proportion being superimposed on the pre-existing welded matrix of the rock preserving phenocrysts of quartz and feldspar, Fe-Ti-Mn oxide aggregates and relict eutaxitic textures (fig. 3E). Concentric growth patterns are common within the lithophysae, usually reflecting an alternation of fine and coarse quartz aggregates or sericite-rich bands. In some cases the banding is accentuated by conformable hematite and pyrite disseminations and dustings (fig. 3D).

*Mineral paragenesis.* The detailed sequence of mineral paragenesis (fig. 4) shows the three major stages in the evolution of the ignimbrites. Stage I represents the primary accumulation, consolidation, and welding of the ash-fall and ash-flow tuffs, and rhyolites. Primary phases include quartz, feldspar (consisting of albite which may be a replacement phase of a primary alkali feldspar), ilmenite, and titanomagnetite (containing exsolved hematite) together with subordinate apatite, sphene, and zircon. As described above, quartz and feldspar are present as partially resorbed phenocrysts in addition to being major matrix constituents. The ilmenite and titanomagnetite, now mostly altered to Fe-Ti-Mn oxides (Stage II), occur dispersed throughout the fabric with a greater density in the unwelded, more tuffaceous, horizons. Apatite occurs sporadically and, together with zircon, is commonly observed peripheral to, but sometimes included within, opaque clusters. Both are also included in feldspar and quartz. The zircons are commonly, but not invariably, zoned and, in addition to their common association with the opaques, they also occur sporadically throughout the rock fabric.

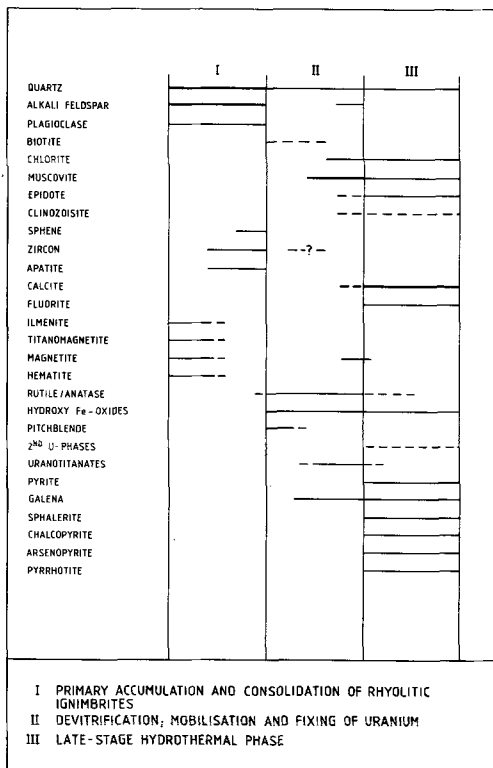


FIG. 4. Paragenetic sequence of mineralization within the Duobblon ignimbrites. Thickness of bars denote the relative abundancies of the mineral phases.

Stage II is characterized by devitrification of the ignimbrites associated with mobilization and reconcentration of U. Devitrification textures, typified by spherulites and lithophysal and vapour-phase cavities, have been described above.

The solutions active during this stage were calcium- and fluorine-rich and oxidizing, resulting in the partial to complete oxidation of ilmenite and titanomagnetite to Fe-Ti-Mn oxide clusters (usually residual ilmenite-titanomagnetite together with rutile, anatase, and leucoxene); the sporadic occurrence of biotite, mainly in the non-welded tuffs, at the expense of the small dispersed Fe-Ti-Mn oxide aggregates, and the precipitation of hydroxy Fe-oxides, often concentrically, within the developing lithophysae, along microfractures and around altering opaque clusters. The Ca enrichment of the fluids resulted in the formation of epidote and clinozoisite, which occasionally rims ilmenite and titanomagnetite.

The precipitation of U as fine granular pitchblende around the Fe-Ti-Mn oxide clusters, and the subsequent breakdown of the pitchblende releasing U to form complex uranotitanates with these oxides, is characteristic of the ignimbrites (Lindroos and Smellie, 1979).

The partial, or complete, alteration of matrix feldspar (and to a lesser extent feldspar phenocrysts) to sericite is generally widespread, especially in the mineralized horizons.

Stage III involves late-stage hydrothermal solutions of low U content but enriched in sulphur. These precipitated sulphides occur mostly in the U-rich horizons of the ignimbrites. The sulphides, consisting in order of relative abundance of pyrite, sphalerite, galena, arsenopyrite, chalcopyrite (accompanied sometimes by bornite and covellite), pyrrotine, and molybdenite occur as matrix impregnations, interstitial cavity and fracture fillings, and with such late-stage phases as calcite, quartz, muscovite, epidote, chlorite, and fluorite.

Epidote, calcite, and muscovite often occur in the partly pseudomorphed feldspar phenocrysts as a later impregnation. These minerals and fluorite tend to be more common in the non-welded tuffs.

Remobilized secondary U concentrations are not common within the ignimbrites, being found only rarely in small fractures mainly in the more porous non-welded tuffs. A sample from the underlying granitic basal breccia has been identified as uranophane (Löfvendahl, 1981).

Galena, which is probably largely radiogenic, occurs as blebs and stringers in pitchblende. A later hydrothermal variety occurs as a vein mineral associated with the sulphides mentioned above.

#### *Some characteristics of the red-bed series*

The rhyolitic ignimbrites are overlain by up to 400 m of thick fluvial deposits of red-bed-type conglomerates and tuffitic sandstones (figs. 1 and 2) which have been described in detail by Einarsson (1970, 1979). Briefly, the red to grey-red tuffitic sandstone (up to 70 m thick) grades from the underlying volcanics into an alternating conglomerate and sandstone sequence. Slip textures, probably formed by slumping of unconsolidated layers, suggest some tectonic activity during sedimentation.

The sandstone consists of fragments of quartz, alkali feldspar, and sericitized plagioclase in a fine sericitized matrix. The matrix consists of aggregates of sphene, epidote, leucoxene, opaque minerals, calcite, and chlorite (fig. 6C). Well-preserved ash textures indicate the pyroclastic nature of the rock.

The polymict conglomerate, consisting mostly of material not represented within the Duobblon area, is conformable on the tuffitic sandstones. The dominant pebble types are of granite and acid volcanic rocks with subordinate sandstone, pelite, basic volcanic rock, and jasper.

Both porphyritic and ignimbritic varieties of volcanic rocks are represented, the later showing clear eutaxitic textures. The finest matrix fractions consist of small angular quartz, alkali feldspar, and plagioclase fragments in a dense tuffitic matrix of sericite, calcite, and epidote with sporadic apatite, zircon, tourmaline, sphene, leucoxene, and opaque minerals (fig. 6A, B).

#### *Chemistry of the ignimbrites*

Samples representative of the top and bottom ignimbrite flows (fig. 2), were selected for major element analysis and the determination of V, Cr, Co, Ni, Cu, Zn, As, Rb, Sr, Y, Zr, Mo, Sn, W, Pb, Bi, Th, and U. The samples were selected on the basis of their background U contents and represent a lateral extent of several kilometres. The analyses are presented in Table II.

The major element analyses indicate that the ignimbrites are calc-alkaline in composition with no significant variation in composition between and within the ignimbrite flows which are separated by thin conglomeratic beds. The distribution of Na<sub>2</sub>O and K<sub>2</sub>O along vertical profiles through the ignimbrite units was investigated although the data are limited. No systematic indications of primary magmatic variations were observed. This may be due to alkali ion exchange between the rock and aqueous phases during devitrification and hydration of the ignimbrite flows, although such processes are considered to be more active for rocks

of peralkaline composition (Lipman, 1965; Noble *et al.*, 1967; Lipman *et al.*, 1969; Scott, 1971; and Zielinski *et al.*, 1977). It is suggested that the original alkaline magmatic trends of the Duobblon ignimbrites have been obliterated and that this has probably been aided by the limited thickness of the flows (approx. 30 m thick).

The U abundance in the unmineralized samples (Table II, excluding the enriched samples 212, 214,

215, 175, and the low-Th sample 216) range from 7.9 to 17.7 ppm U compared to 2 to 10 ppm U for acid igneous rocks generally (Rogers and Adams, 1969). If the elevated U contents are primary they suggest a relatively late-stage development of the ignimbrites in the magmatic evolution of the region. However, mobilization and reconcentration of U during devitrification is assumed to have been an important feature of the ignimbrites. The

TABLE II: Chemical analyses of ignimbrites from Duobblon, N. Sweden.

	BUAJ 207	BUAJ 208	BUAJ 209	BUAJ 210	BUAJ 211	BUAJ 212	BUAJ 213	BUAJ 214	BUAJ 215	BUAJ 216	BUAJ 217	BUAJ 218	BUAJ 233	BUAJ 234	BUAJ 235	BUAJ 237	BUAJ 175	BUAJ 144
SiO <sub>2</sub>	77.6	74.7	76.8	74.9	68.5	70.4	74.3	77.6	77.2	67.9	70.1	69.3	68.5	71.1	74.3	75.5	76.7	76.2
TiO <sub>2</sub>	0.19	0.19	0.22	0.21	0.20	0.24	0.21	0.18	0.19	0.46	0.24	0.22	0.22	0.27	0.21	0.23	0.22	0.21
Al <sub>2</sub> O <sub>3</sub>	12.4	12.6	12.9	13.1	16.2	15.5	12.9	12.7	12.6	17.6	14.8	13.4	16.5	15.2	14.1	13.4	13.3	12.0
Fe <sub>2</sub> O <sub>3</sub>	0.6	0.9	1.9	1.8	1.4	0.9	1.4	0.9	0.9	2.2	1.9	1.0	1.1	0.6	0.9	0.8	1.1	0.4
FeO	0.7	1.2	0.5	0.5	0.8	1.1	0.9	0.8	0.5	1.8	0.3	0.5	0.8	1.4	1.2	1.3	0.4	0.9
MnO	0.02	0.03	0.02	0.02	0.07	0.03	0.03	0.02	0.02	0.04	0.01	0.03	0.02	0.04	0.06	0.03	0.02	0.02
CaO	0.4	0.9	0.3	0.3	0.8	0.6	0.4	0.3	0.4	0.7	0.2	0.2	0.2	0.3	1.1	0.4	0.3	0.3
MgO	0.27	0.21	0.23	0.35	1.72	0.55	0.25	0.22	0.18	1.19	0.25	6.5	0.31	0.27	1.03	0.21	0.28	0.23
Na <sub>2</sub> O	1.8	2.1	1.1	0.7	1.9	1.5	2.5	0.9	1.2	0.7	1.2	0.8	0.7	3.0	3.6	0.7	1.4	1.6
K <sub>2</sub> O	5.7	5.8	6.4	6.2	5.1	7.9	6.1	6.9	6.4	5.4	7.6	6.8	8.7	6.5	2.5	6.7	6.3	7.9
H <sub>2</sub> O <sup>+</sup>	1.0	0.7	1.2	1.3	1.6	1.1	0.8	0.8	0.3	2.2	0.6	0.9	1.3	1.0	1.2	1.2	0.9	1.4
H <sub>2</sub> O <sup>-</sup>	<0.1	<0.1	<0.1	<0.1	<0.1	<0.1	<0.1	<0.1	<0.1	<0.1	<0.1	<0.1	<0.1	<0.1	<0.1	<0.1	0.3	0.2
P <sub>2</sub> O <sub>5</sub>	0.03	0.02	0.03	0.03	0.02	0.04	0.02	0.03	0.17	0.06	0.04	0.04	0.04	0.04	0.03	0.03	0.06	0.02
CO <sub>2</sub>	0.18	0.50	0.01	0.02	0.16	0.25	0.12	0.12	0.18	0.32	0.18	0.15	0.01	0.05	0.51	0.10	0.17	0.20
F	0.04	0.03	0.04	0.05	0.22	0.07	0.03	0.03	0.04	0.13	0.05	0.04	0.08	0.04	0.08	0.05	0.05	0.11
S	0.14	0.02	0.02	0.02	0.02	0.04	0.02	0.14	0.11	0.02	0.95	0.09	0.18	0.03	0.02	0.20	0.08	0.02
BaO	0.03	0.02	0.04	0.03	0.03	0.05	0.03	0.04	0.04	0.11	0.04	0.05	0.04	0.03	0.04	0.05	0.04	0.03
	101.20	100.02	101.81	99.63	98.84	100.37	100.11	101.78	100.53	100.93	98.56	100.12	98.80	99.97	100.98	101.00	101.62	100.74
V †	64	58	28	30	19	207	33	272	310	112	291	65	79	21	10	43	50	94
Cr †	5	6	5	6	11	6	7	6	10	52	6	6	5	5	5	5	5	7
Co †	<10	<10	<10	<10	<10	<10	<10	<10	<10	<10	<10	<10	<10	<10	<10	<10	<10	<10
Ni †	0	0	0	1	0	0	0	0	0	13	3	0	4	1	0	0	2	12
Cu †	9	18	7	6	6	11	22	11	10	5	8	8	12	7	12	16	7	34
Zn †	11	117	41	42	57	38	45	29	105	73	28	28	53	26	62	189	11	48
As †	<50	<50	<50	<50	<50	<50	<50	<50	<50	<50	263	<50	87	<50	<50	<50	<50	<50
Rb †	219	273	294	285	277	287	286	309	291	253	229	269	307	235	147	271	345	177
Sr †	72	111	73	91	181	135	77	80	96	59	143	89	112	81	203	96	112	194
Y †	51	68	66	67	63	62	70	74	67	45	56	71	65	50	54	69	136	97
Zr †	416	422	434	417	530	476	443	403	406	397	461	455	485	536	472	446	318	305
Mo †	<10	<10	<10	<10	<10	<10	<10	<10	<10	<10	29	<10	<10	<10	<10	<10	<10	<10
Sn †	6	11	10	14	17	12	12	12	16	<5	14	15	15	9	11	10	<5	6
W †	0	0	2	4	0	0	0	6	10	0	3	9	7	4	2	0	0	0
Pb †	13	38	16	12	15	31	17	61	148	14	31	14	37	12	10	80	74	31
Bi †	<5	<5	<5	<5	<5	<5	<5	<5	<5	<5	<5	<5	<5	<5	<5	<5	<5	<5
Th •	29.5	35.4	35.5	35.6	33.7	31.1	35.3	38.8	29.8	14.6	27.4	39.0	36.5	25.8	31.1	34.1	40.4	40.9
U x	14.8	16.2	15.2	17.2	8.0	135	12.2	317	648	7.9	33.2	15.9	17.7	12.2	15.2	13.3	501	17.1
eU •	17.2	15.0	14.2	13.6	6.9	139	11.0	297	605	5.9	26.7	14.0	15.5	9.6	14.2	10.6	476	14.1
Th/U	1.99	2.18	2.34	2.07	4.21	0.23	2.89	0.12	0.05	1.85	0.82	2.45	2.06	2.11	2.05	2.56	0.08	2.39
eU/U	1.16	0.93	0.93	0.79	0.86	1.03	0.90	0.94	0.93	0.75	0.80	0.88	0.88	0.79	0.93	0.80	0.95	0.82

† Analysis by optical emission spectrometry

‡ Analysis by X-ray fluorescence

x Analysis by delayed neutron activation (DNA)

• Analysis by sealed-can gamma-ray spectrometry (eU is the equivalent uranium content)

Trace element analysis are presented as parts per million (ppm).

Major elements including total Fe were analysed by XRF. Fe<sup>2+</sup>;

Na<sub>2</sub>O; H<sub>2</sub>O<sup>+</sup>; H<sub>2</sub>O<sup>-</sup>; H<sub>2</sub>O; P<sub>2</sub>O<sub>5</sub>; CO<sub>2</sub>; F and S were analysed by standard wet chemical techniques.

Analysis of sample 175 and 144 are from Lindroos and Smellie (1979).

eU/U ratios indicate that within recent geological time little significant remobilization of U has occurred. This is confirmed by the lack of secondary U precipitation.

Other elements which might reflect remobilization include Mo, F, and Cl (Shatkov *et al.*, 1970; Haffty and Noble, 1972). Mo contents (Table II) are, with one exception, less than 10 ppm which is close to the average value for rhyolitic rocks (1–5 ppm Mo). Within the Duobblon rhyolitic ignimbrites as a whole, however, sporadic enrichments of up to 70 ppm Mo occur although these do not necessarily coincide with U enrichments. In one case 2000 ppm Mo was determined from a section containing 241 ppm U, the Mo occurring as finely disseminated molybdenite. Molybdenite associated with pyrite impregnations has been found in U-enriched boulders of quartz porphyry from the Gippervare Formation (Ö. Einarsson, pers. comm.). It appears, therefore, that Mo has also been remobilized and concentrated locally, sometimes with U, at various levels in the volcanic pile.

#### *Fission-track studies of U distributions*

Studies were made on a suite of samples collected from the ignimbrites and several samples from the overlying tuffitic sandstones and polymict conglomerates. Polished thin sections were irradiated at the Research Reactor, Studsvik, to study the  $^{235}\text{U}$  fission-track distributions. The tracks were registered on a polycarbonate lexan plastic and subsequently etched according to the method of Kleeman and Lovering (1967).

The U distributions in the ignimbrites (fig. 5) can be summarized as follows:

*Primary accessory mineral phases.* U was located in zircon, apatite, and sphene but not in ilmenite and titanomagnetite.

*Primary major mineral phases.* Quartz and plagioclase contained no U, apart from that introduced along fractures and alteration zones.

*Secondary mineral phases.* Fe–Ti–Mn oxides are largely responsible for the high-density spot concentrations within the matrix. As discussed by Lindroos and Smellie (1979), granular pitchblende is commonly associated with these Fe–Ti–Mn oxide clusters, leading to the incorporation of U into the secondary oxides to form a series of complex uranotitanates.

*Muscovite.* Sericite is present as a major alteration product and fine U disseminations are associated with it, probably as molecular coatings. Matrix sericite is therefore responsible for the 'background' track densities in the examined sections. The coarse muscovite flakes, present as cavity and late-stage fracture infillings, contain no U.

*Late-stage, low-temperature mineral phases.* Small fracture and lithophysal cavity infillings containing varying amounts of chlorite, calcite, epidote, fluorite, and sulphides, mostly contain no U. Matrix pyrite sometimes has U coatings and cavity chlorite may include discoloration haloes associated with weak track densities possibly reflecting the occurrence of grains ( $< 10 \mu\text{m}$ ) of hydrothermal zircons.

Fission-track studies of tuffitic sandstone and polymict conglomerates (fig. 6) show that U is associated with epidote, apatite, zircon, sphene, Fe–Ti–Mn oxides (usually as rutile–anatase–leucosene aggregates), chlorite, hematite, hydroxy Fe-oxides, and matrix sericite. Track densities are similar to those observed in the ignimbrites. Mineral phases with negligible U contents included quartz, potash feldspar, plagioclase, and biotite.

#### *Genetic considerations and discussion*

The primary U host minerals (apatite, sphene, and zircon) of the Duobblon rhyolitic ignimbrites are not sufficiently abundant to contribute significantly to the total U in the rock. Chemical studies show that the ignimbrites are calc-alkaline and are enriched in U, with associated stratabound mineralization containing more than 4000 tonnes of U with an average content of 0.03 % U (Lindroos, 1980).

It is suggested that oxidizing uraniferous solutions pervaded the ignimbrites with the greatest percentage of U being reprecipitated as pitchblende and complex uranotitanates associated with Fe–Ti–Mn oxides, and as coatings associated with matrix sericite. The Duobblon rhyolitic ignimbrites are therefore enriched in U compared to normal rhyolites, and thus the primary U contents of the rhyolites and tuffs, and the extent of U mobilization during post-depositional devitrification and recrystallization, cannot be determined accurately.

The mobilization and leaching of U during devitrification and recrystallization of volcanic glasses to form felsites has been demonstrated previously by Rosholt and Noble (1969), Shatkov *et al.* (1970), Zielinski (1978), and Zielinski *et al.* (1980). Work by Zielinski (1978) has shown that the U abundance in obsidians can range from 5 to 46 ppm U, as compared to 2 to 10 ppm U for normal granites and rhyolites (Rogers and Adams, 1969). Rosholt and Noble (1969) and Zielinski (1978) have indicated that up to 80 % of U can be lost during crystallization of acid volcanic rocks. As suggested by Lindroos and Smellie (1979), significant amounts of U in the Duobblon ignimbrites could have been present in the groundmass of the rock during deposition, and subsequently mobilized and fixed during devitrification.

It is possible, however, that U has been introduced into and lost from the ignimbrites at different times. Local enrichments of 100 to 1000 ppm U occur in the overlying conglomerates although the tuffitic sandstones are relatively homogeneous with respect to U. Fission-track studies show that uraniferous solutions affected the conglomerates and sandstones and that quantities of U were fixed in a similar fashion to those described for the ignimbrites. Moreover, the conglomerates and sandstones are capped by acid volcanics of ignimbrite character (the Gippervare Formation; figs. 1 and 2), which also contain several small U concentrations, so that the Duobblon group represents a considerable thickness (approx. 2400 m at the present erosional level) of rocks and sediments which are largely derived from volcanic material. They thus represent a large potential source of U in which oxidizing solutions have remobilized and concentrated U. The widespread sericitization throughout the Duobblon group provides additional evidence of large-scale movement of solutions through the volcanic pile, probably during consolidation and devitrification of the volcanics and during diagenesis of the sediments. It is suggested that U was transported as uranyl carbonates and, to a lesser extent, uranyl fluoride complexes. However, hexavalent U is readily leached from rhyolites by dilute acid solutions so some U may have been transported as  $\text{UO}_2(\text{OH})^+$  and  $\text{UO}_2^-$  complexes.

The ignimbrites thus appear to have provided a 'sink' for U from solutions percolating through fractures, fissures, and more permeable, less-welded layers and lenses. Thus the highest U, and later sulphide, occurrences are located along more permeable zones provided by the large lithophysal horizons. Similar observations have been described

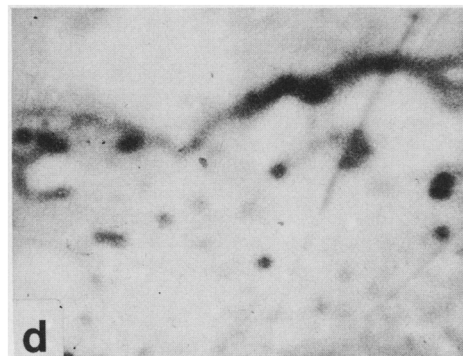
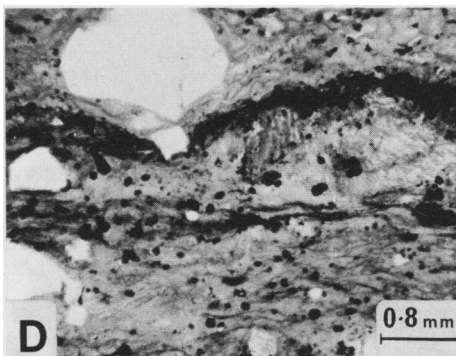
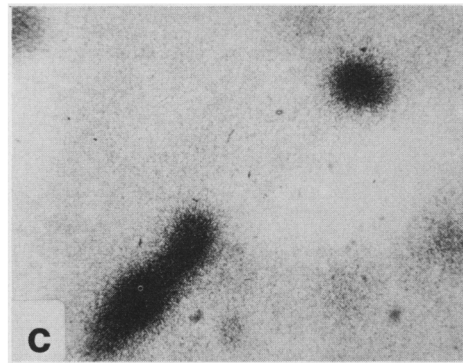
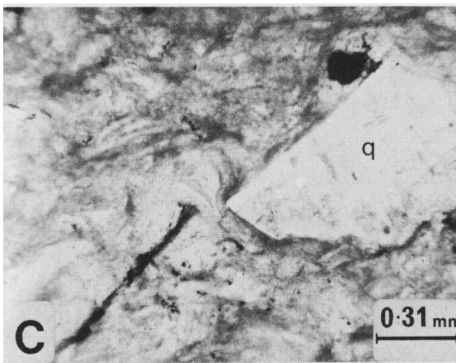
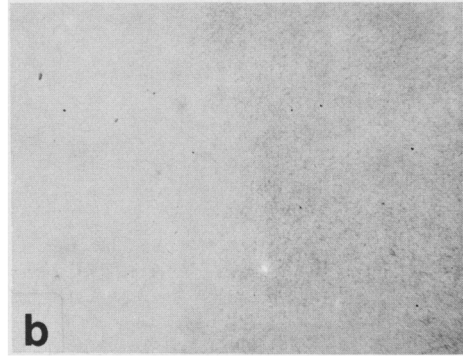
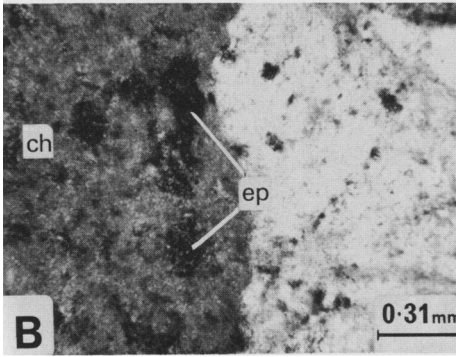
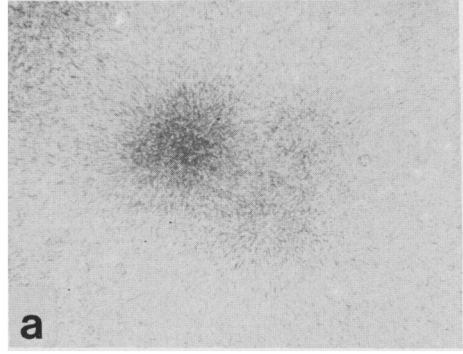
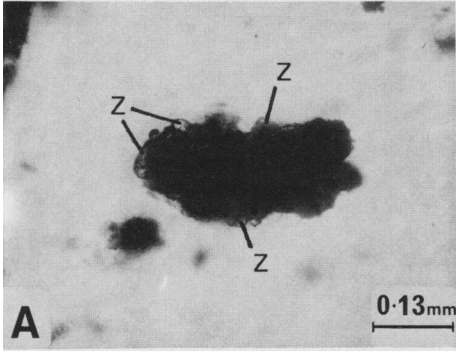
from the Buckshot Ignimbrites by Andersson (1975) who noted that the strongly altered lithophysal zone was the most reliable indicator of significant U mineralization. Unfortunately little published information is available for the Italian Novazza mine.

In Duobblon, the precise processes of U (and minor sulphide) precipitation are not yet clear. There is no evidence of hydrothermal sulphide enrichments prior to the introduction of uraniferous solutions to provide a redox barrier for U precipitation. However, the higher U concentrations can be partly explained by the greater abundance of Fe-Ti-Mn oxides with a greater density of possible precipitation sites for U. Furthermore, the greater permeability and porosity of these horizons contributed to the high degree of hydrothermal alteration, and hence U enrichment associated with sericite. The rock matrix is often charged with small euhedral to subhedral magnetite grains partly martitized to hematite which have been suggested (Lindroos and Smellie, 1979) to be due to expulsion of iron compounds during formation of the lithophysae. These may have assisted in the precipitation of U and later sulphides.

*Acknowledgements.* Thanks are due to Dr H. Lindroos for providing material from Duobblon and for his constructive comments on the manuscript. Drs Ö. Einarsson and U. Hålenius (Luleå) and B. Levi (Stockholm) critically read and improved the manuscript. The whole-rock and trace element analyses were performed by the Swedish Geological Survey Laboratory, Luleå. The neutron activation analyses and fission-track irradiations were carried out at Studsvik Energiteknik AB, Sweden, and the gamma-ray spectrometry analyses were carried out at the Danish Atomic Energy Commission Research Establishment at Risø, Denmark.

---

FIG. 5. Fission-track distributions from the Duobblon ignimbrites. A. Rutile-anatase-leucoxene alteration products resulting from the oxidation of primary titanomagnetite. a. The fission-track densities are related to the peripheral primary zircons (Z). Unmineralized specimen; plane polarized light. Specimen BUAJ 154. b. Interior of a large lithophysa showing the contact between the central cavity, infilled with Fe-rich chlorite (ch) and epidote aggregates (ep), and the lithophysal interior composed mainly of felsite with finely dispersed sericite. b. The fission-track density is controlled by the sericite distribution; the late-stage cavity infilling material is devoid of any U. Unmineralized specimen; plane polarized light. Specimen BUAJ 155. c. Quartz phenocryst set in a welded matrix composed of glass shard eutaxitic textures, some suggesting flow structures; the matrix is heavily sericitized. c. The fission-track density is particularly marked along a thin fissure and from one aggregate, both of which contain Fe-Ti-Mn oxides (now mostly rutile-anatase-leucoxene) together with finely dispersed pitchblende and sporadic zircons. Mineralized specimen; plane polarized light. Specimen BUAJ 164. d. Less-welded tuff characterized by quartz and feldspar phenocrysts set in a fine granular matrix which is sericitized and impregnated with magnetite and Fe-Ti-Mn oxides. The section is traversed by a small fissure infilled mostly with Fe-Ti-Mn oxides, disseminated pitchblende, and sporadic zircons. d. The high fission-track densities relate to altered Fe-Ti-Mn oxides (together with finely dispersed pitchblende) often with associated zircons. The lower density throughout the section is due to the matrix sericite. Note the absence of tracks from the quartz and feldspar phenocrysts. Mineralized specimen; plane polarized light. Specimen BUAJ 154.



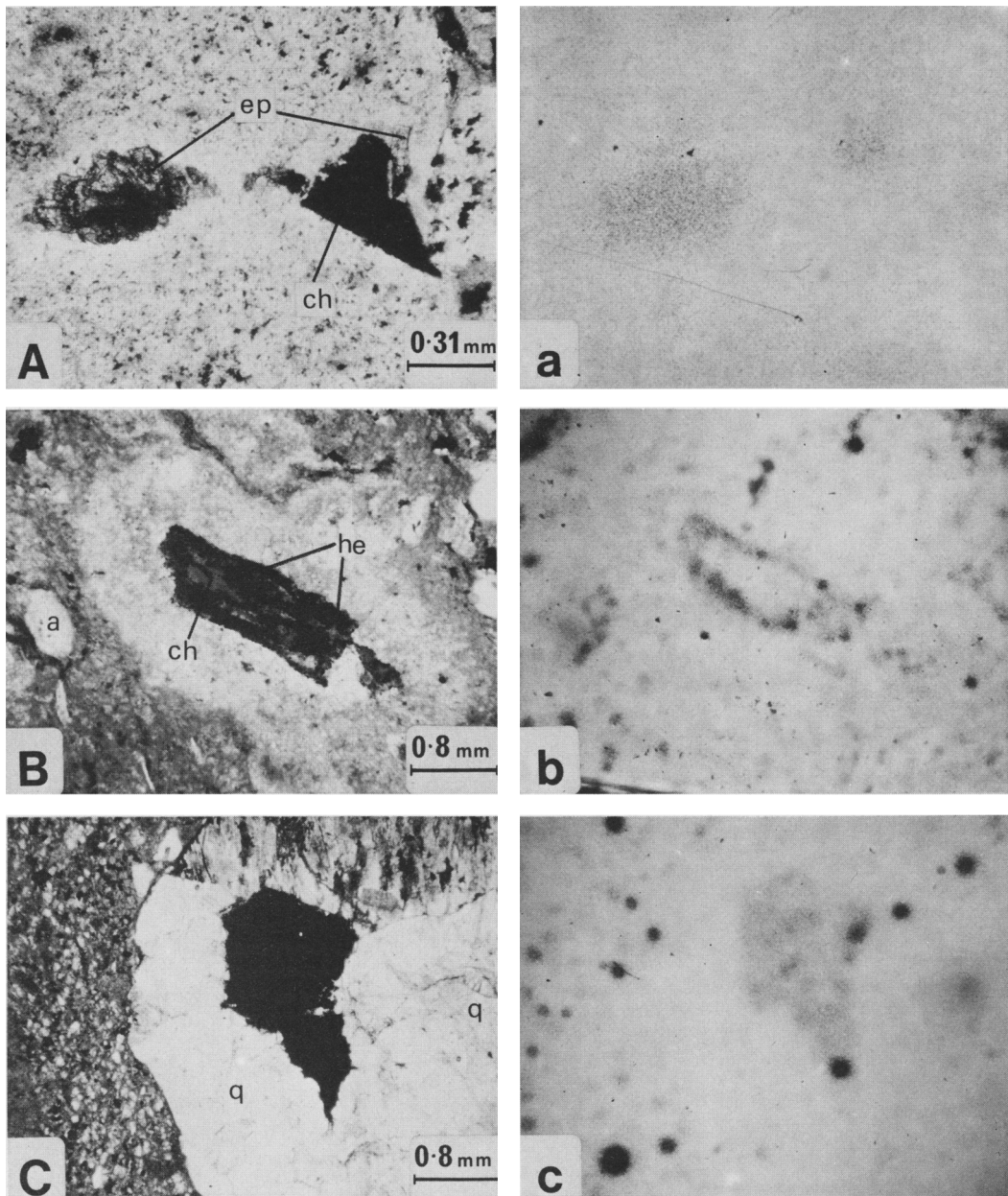


FIG. 6. Fission-track distributions from the conglomerates (A, B) and sandstones (C). A. Aggregates of epidote (ep) and a chloritic pseudomorph (ch) contained within a felsitic volcanic fragment rich in matrix sericite. *a*. The fission-track density relates mostly to the epidote (intermediate track density) and matrix sericite (low background track density). Unmineralized specimen; plane polarized light. Specimen BUJ 160. B. Chlorite pseudomorph after biotite; marginal to and penetrating the chlorite (ch) is hematite (he). Surrounding the pseudomorph is a zone composed of felsite and devoid of mafic constituents. Peripheral to this zone is an apatite grain (a) and small quartz fragments set in a felsite matrix which is rich in disseminated sericite and chlorite. *b*. Intermediate track densities are associated with hematite, apatite, and the matrix sericite and chlorite. Points of high track density throughout the section relate to sporadic zircon grains and Fe-Ti-Mn oxides. Mineralized specimen; plane polarized light. Specimen BUJ 180. C. Opaque aggregate partly enclosed by a quartz mosaic (q); the surrounding matrix is tuffitic in character and rich in chlorite and sericite. The opaque phase consists mainly of hematite with associated chlorite and sporadic Fe-Ti-Mn oxide aggregates. *c*. The intermediate track density is relatively uniform within the opaque mass with points of high track density throughout the section correlating with Fe-Ti-Mn oxides and zircon grains. The matrix low track density background is due mostly to sericite, and the granular texture of the quartz, marginal to the opaque, has facilitated the penetration of U disseminations along grain boundaries. Weakly mineralized specimen; plane polarized light. Specimen BUJ 228.

## REFERENCES

- Adamek, P., and Wilson, M. R. (1979) *Proc. R. Soc. Lond.* **291**, 355-68.
- Anderson, W. B. (1975) Unpubl. MA thesis, University of Texas, Austin.
- Einarsson, Ö. (1970) Unpubl. Ph.D. thesis, University of Stockholm.
- (1979) SGU, Ser. C. 748.
- Guarascio, M. (1976) *Improving the uranium deposits estimations (the Novazza case)*. In NATO advanced study institute series, ser. C, mathematical and physical sciences. *Advanced geostatistics in the mining industry*, D. Reidel Publ. Co., Dordrecht, Holland. 351-67.
- Haffty, J., and Noble, D. C. (1972) *Econ. Geol.* **67**, 768-75.
- Kleeman, J. D., and Lovering, J. F. (1967) *Science*, **156**, 512-13.
- Lilljequist, R., and Svensson, S-Å (1974) *Geol. För. Stockh. Förh.* **96**, 221-9.
- Lindroos, H. (1980) Int. Rep. SGU.
- and Smellie, J. A. T. (1979) *Econ. Geol.* **74**, 1118-30.
- Lipman, P. W. (1965) *US Geol. Survey Bull.* 1201-D.
- Christiansen, R. L., and Van Alstine, R. E. (1969) *Am. Mineral.* **54**, 286-91.
- Löfvendahl, R. (1981) SGU, Ser. C. 779.
- Noble, D. C., Smith, V. C., and Peck, L. C. (1967) *Geochim. Cosmochim. Acta*, **31**, 215-23.
- Rogers, J. J. W., and Adams, J. S. S. (1969) *Uranium*. In Wedepohl, K. H., ed. *Handbook of geochemistry*, 4. New York, Springer-Verlag.
- Rosholt, J. N., and Noble, D. C. (1969) *Earth. Planet. Sci. Lett.* **6**, 268-70.
- Prijana, and Noble, D. S. (1971) *Econ. Geol.* **66**, 1061-9.
- Ross, C. S., and Smith, R. L. (1961) *US Geol. Survey Prof. Paper* 366. 81 pp.
- Scott, R. B. (1971) *J. Geol.* **79**, 100-10.
- Shatkov, G. A., Shatkova, L. N., and Guschin, E. N. (1970) *Geochem. Int.* **7**, 1051-63.
- Welin, E. (1980) *Geol. För. Stockh. Förh.* **101**, 309-20.
- Einarsson, Ö., and Nilsson, Ö. (1971) SGU, Ser. C. 666.
- Zielinski, R. A. (1978) *Geol. Soc. Am. Bull.* **89**, 409-14.
- Lipman, P. W., and Millard, H. T., Jr. (1977) *Am. Mineral.* **62**, 426-37.
- Lindsey, D. A., and Rosholt, J. N. (1980) *Chem. Geol.* **29**, 139-62.

[Revised manuscript received 4 January 1982]